Simulation Of Passively Safe Inspection Trajectories For Non-Cooperative Space Rendezvous

Ksenia Klionovska [(1)], Leo Renaut [(1)], Florian Rems [(1)]

[(1)] German Aerospace Center, Muenchenerstr. 20, 82234, Wessling, Germany,
Email:{ksenia.klionovska; leo.renaut; florian.rems}@dlr.de

***Abstract*—The escalating accumulation of space debris in Earth orbit presents a significant challenge for space operations, threatening both current satellites and future missions. This issue motivated different international scientific communities and industrial sectors to create efficient strategies for its mitigation. This work explores the design of passively safe inspection trajectories for On-orbit Servicing and Active Debris Removal missions. Optimizing the inspection process requires balancing several factors, including target visibility, fuel consumption (ΔV budget), and other mission constraints. The presented inspection trajectories are validated via a high-fidelity software in the loop rendezvous simulator.**

I. Introduction

Far-range rendezvous is one of the main phases of proximity operations in the context of On-Orbit Servicing (OOS) / Active Debris Removal (ADR). The chaser spacecraft approaches the target from tens of kilometers to a few hundred meters by several impulsive maneuvers. At this point, an inspection is what usually follows, regardless of what activity is planned (e.g. a lifespan extension, refueling or removal) [2]. The servicer should provide the data necessary to assess the target's condition. It may include collecting visual data (images or point clouds) for further on-ground processing. This data analysis helps to reconstruct the target's shape, to assess damages and anomalies, to estimate the initial orientation and spinning rate before the OOS mission proceeds.

Commercial as well as government organizations focus on orbital inspection and servicing. The goal of the ADRAS-J mission is to safely approach, characterize and fly around a large piece of space debris in Low Earth Orbit (LEO). The target's spin rate and axis are planned to be determined from the inspection data. [4], [3]. The company True Anomaly intends to demonstrate proximity operations and inspection, including gathering of visual information [5]. DARPA's Robotic Servicing of Geosynchronous Satellites (RSGS) program [6] and Mission Extension Vehicle (MEV) [7] are focused on OOS tasks with a target satellite in GEO orbit.

Due to the growing need for such missions, there is a big demand on research and on-ground simulation of autonomous operations that can ensure a safe approach and fly-around. In particular, a careful analysis of relative inspection trajectories that are guaranteed to be collision-free, even when facing a loss of control or other possible anomalies, is necessary for every mission. In [10] and in [11], the authors present inspection trajectories in the form of Walking Safety Ellipses (WSE) with different widths for a small target. In [12], simulations of parametric models for periodic relative orbits for visual inspection of the Chinese Space Station with a CubeSat are performed. Theoretically, this approach can also be applied for rendezvous with uncooperative targets.

In contrast to close range operations, Guidance, Navigation and Control (GNC) systems for either far-range rendezvous or inspection cannot be directly tested with hardware-in-the-loop (HiL) facilities, e.g. the European Proximity Operations Simulator (EPOS)[8] or NASA's Johnson Space Center high-fidelity Rendezvous, Proximity Operations and Docking (RPOD) [9]. Therefore, at DLR's OOS group we have begun to implement a software-in-the loop (SiL) far-range simulator. By incorporating different software components with realistic models of spacecraft dynamics, external perturbations, and visual sensor characteristics, this tool allows to model, refine and tune safe trajectories for inspection and proximity operation in a virtual environment. This simulator is built with the experience of DLR in the Prototype Research Instruments and Space Mission Technology Advancement (PRISMA) mission [14] and the Autonomous Vision Approach Navigation and Target Identification (AVANTI) [13] experiment. More details about the far-range simulator will be provided in the next Section II-B.

This paper focuses on the simulation of passively safe inspection trajectories of a target in Low Earth Orbit (LEO). The key aim is to establish trajectories which allow the chaser spacecraft to visualize the target from different viewpoints, while minimizing the consumption of ΔV and keeping a safety margin distance between chaser and target. The results of simulation are presented in Section III.

II. Methods

A. Inspection mission phases

This section begins with the design of an OOS mission, primarily focused on the inspection of the target spacecraft. The main stages of the mission are depicted in Fig. 1, with further explanations provided below.

- **Launch and Early Orbit Phase (LEOP) / Transfer**. This phase covers activities from the launch of the servicing spacecraft until it begins the far-range approach. The servicer satellite is released as a payload from the launcher and completes several tasks (e.g. system checks, deployment of solar panels and antennas). Using absolute navigation information, the chaser performs orbital transfer maneuvers commanded from the ground to move from the launcher's initial orbit to the target's one.
- **Far-rendezvous**. The beginning of far-range rendezvous involves the switch from absolute to relative navigation.

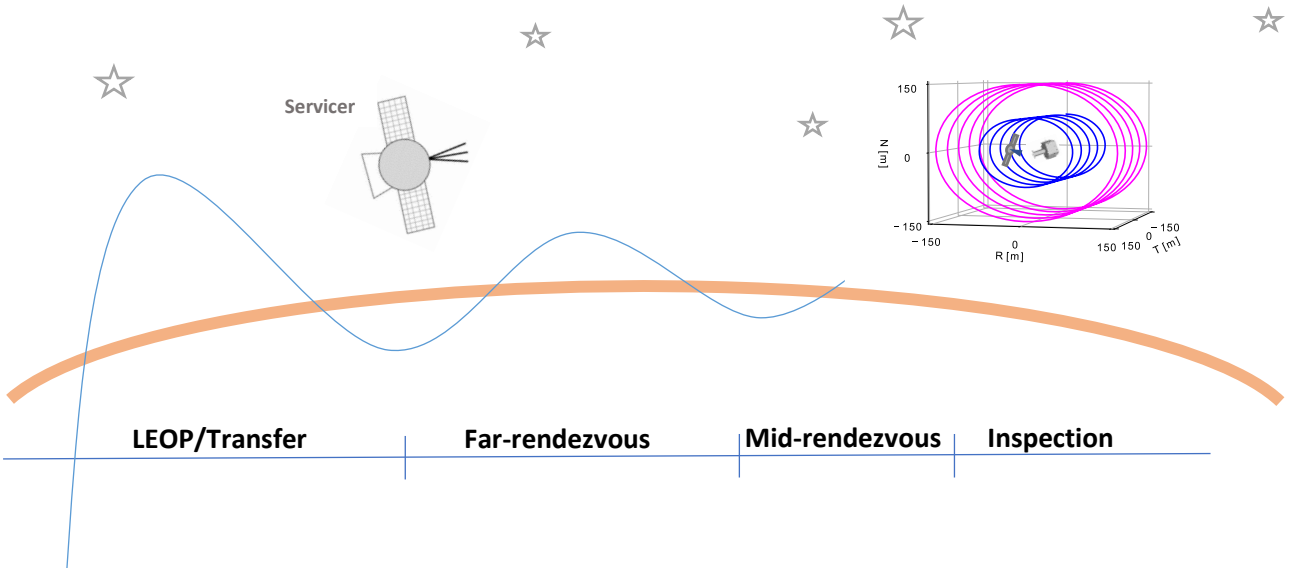

Fig. 1. The main stages of an OOS mission, with a primary focus on inspection

This stage can be started as soon as the target becomes visible in the far-range visual sensor - in the AVANTI experiment this was the case at 40 km [1] and in PRISMA mission at 30 km [15]. The rendezvous involves the servicer gradually approaching the target.

- **Mid-rendezvous**. During the mid-range rendezvous phase, the servicing spacecraft closes in on the target spacecraft, transitioning from far-range to proximity operations. This phase can include some other different accurate sensors for visual navigation. As for example, Lidar sensors for the precise distance measurements and high-resolution optical cameras for capturing detailed images.
- **Inspection**. After the servicing spacecraft has safely approached a target, inspection maneuvers can be initiated. In this paper, we intend to gradually reduce the width of Walking Safety Ellipses (WSE) within the Radial-Normal (RN) plane of the Radial-Tangential-Normal (RTN) frame, aiming to achieve a small and safe relative distance between the chaser and target for a close fly-around maneuver. In the Fig. 1, a sketch of such WSEs with a width of 300 m (blue) and 150 m (magenta) is presented.

In the rendezvous/inspection scenarios discussed in this work, the chaser is solely responsible for maneuvering and ensuring the mission's success, while the target spacecraft remains passive. In order to accurately simulate the realistic proximity and inspection trajectories in the orbits discussed above, the following subsection introduces the SiL far-range simulator.

B. Far-range rendezvous simulator

The far-range simulator consists of several key components. The complete simulation environment is implemented in C++, with the final goal to migrate the evaluated GNC components to onboard systems. The most important parts are described below. It should be noted that mathematical calculations are not included in the description of the far-range simulator. To get a deeper understanding of the theory, the authors ask to look at the listed references.

- **Relative Motion Dynamics**. The high-fidelity 6DOF dynamics simulator is used to propagate the position and attitude of a satellite with different external forces (Earth gravity field including harmonic perturbations until the 20^{th} order, aerodynamic drag, Sun and Moon attraction effects and solar radiation) as described in [16]. For the simulation of the chaser's absolute motion it also considers control forces and torques.
- **Line-of-sight measurements**. At the moment, Line-of-sight (LOS) measurements for the angles-only navigation are simulated from true measured states of chaser and target by adding some noise. One of these noisy unit vectors represent the direction to the target in the orbital frame of the chaser. Sun exclusion angles are considered during the whole simulated mission phases, and if the field-of-view (FOV) of a far-range camera sensor is blinded by the Sun, no LOS measurements are generated. Also, no LOS measurements are provided to the filter if the satellite is in Earth's shadow, or if the Earth is in the sensor's FOV.
- **Lidar simulator**. In close range to the target (typically below a few hundred meters), additional measurement from e.g. a lidar sensor can be simulated. A high-fidelity lidar point cloud simulator has been developed to generate 3D point clouds of the target. This simulator enables to develop algorithms for 3D point cloud processing [21]. However, the lidar sensor is not used in the experiments presented in this work, which rely on angles-only navi-

gation using LOS measurements.

C. GNC system

- **Navigation Solution**. The problem of relative orbit determination involves estimating the position and velocity (the relative state) of a target satellite in relation to a servicer at a certain moment, using observational data. Usage of camera, in both cases for far-range and mid-range rendezvous, allows to get angles-only measurements in form of azimuth and elevation angles. The chaser is controlled to be in a target pointing mode, where the boresight of the camera is pointing at the target, while minimizing the angle between the solar panels and the Sun. For the moment, the line-of-sight measurements are simulated as detailed in Section II-B.
  The implementation of the navigation approach for far-range simulation is based on the methods described in the papers [1] [17]. The Extended Kalman filter (EKF) is used to determine the relative state with a set of line-of-sight (LOS) unit vectors. The filter is processing observations sequentially, adapting to new information about the target as it becomes available. This approach progressively improves the accuracy of the relative states over time. When transitioning from far-range to mid-range distance and during inspection, the same filter can be used to process additional 3D position measurements from a Lidar sensor. However, in this work, only line-of-sight measurements are used for the rendezvous.
- **Guidance and Control**. The objective of the relative orbit guidance and control is to compute the impulsive maneuvers necessary to achieve a desired state within a fixed time. To this aim, the relative motion is described using relative orbital elements (ROE) with incorporated impact of J_2 and differential air drag effects into the relative orbital dynamics [19]. The maneuvering is limited by the fact that there might be time intervals where no maneuvers are possible, by the minimum and maximum capabilities of the thrusters as well as the ones of the reaction wheels.
  The guidance minimizes the ΔV consumption to reach the desired state, while always keeping a minimum cross-track separation (safety) margin [20]. The relative orbital guidance and control solution which was in charge of the AVANTI mission is implemented in our far-range simulator. A description of the maneuver planning algorithm implemented by the simulator is in [18]. Firstly, a number of discrete intermediate steps (waypoints) is defined in order to perform the transition from the current state to the final one as in Equation 5 of [13]. The user defines times, at which these waypoints must be reached. Thereafter, a closed-form analytical solution suitable for onboard implementation is proposed to determine a series of impulsive maneuvers which will enable to reach each waypoint. Between each waypoint, 4 impulses are computed (three tangential and one in the normal direction) in order to perform a transition from one state to another. The maneuver planning algorithm allows tuning up several parameters, as e.g. its number of maneuvers, their magnitude, direction and execution times [13].

D. Relative orbital elements

We briefly introduce the relative orbital elements that will be used to define the relative orbit configurations between the chaser and target satellite. The absolute mean orbital elements can be defined by the six elements $(a, e, i, \Omega, \omega, u)$, where a is the semi-major axis, e the eccentricity, i the inclination, Ω the longitude of the ascending node, ω the argument of periapsis and u the mean argument of latitude. Additionally, the eccentricity vector is $\boldsymbol{e} = (e_x, e_y)^T = (e\cos\omega, e\sin\omega)^T$.

Using the subscript "d" for the orbital elements of the target (or "deputy"), the unscaled relative orbital elements (ROEs) are defined in [19] as

$$\begin{pmatrix} \delta a \\ \delta\lambda \\ \delta i_x \\ \delta i_y \\ \delta e_x \\ \delta e_y \end{pmatrix} = \begin{pmatrix} (a_d - a)/a \\ u_d - u + (\Omega_d - \Omega)\cos i \\ i_d - i \\ (\Omega_d - \Omega)\sin i \\ e_{x_d} - e_x \\ e_{y_d} - e_y \end{pmatrix}. \tag{1}$$

The ROE vector is then usually scaled by the semi-major axis a.

III. Results and Discussion

The far-range rendezvous simulator described in Section II-B enables to validate the design of ΔV efficient inspection trajectories in LEO orbits. In the current paper, we consider an exemplary use case involving a satellite in a Sun-synchronous LEO orbit. This orbit type ensures consistent solar illumination during daytime, making it ideal for Earth observation satellites that require stable lighting conditions for optimal operation. Parameters of the target and its orbit are listed in Tab. I.

TABLE I
Target's and orbital parameters used for simulation

Mass [kg]	250
Altitude [km]	550
Inclination [deg]	97,5
Ballistic coefficient [m^2/kg]	0.0208

The initial position and velocity vectors, as well as the initial epoch of the target spacecraft are defined in a configuration file. This information is used for simulation, but unknown to the GNC system which will be tasked with estimating the relative orbit. The chaser mass in this scenario of the simulation is set to 120 kg, with a ballistic coefficient $C_B = 0.0044$ m^2/kg. The field-of-view of the simulated camera is 20×20 deg.

The initial configuration of the two satellites is described using the relative orbital elements of Eq. 1, and is

$$\begin{pmatrix} a\delta a \\ a\delta\lambda \\ a\delta i_x \\ a\delta i_y \\ a\delta e_x \\ a\delta e_y \end{pmatrix} = \begin{pmatrix} -35 \\ 10000 \\ 240 \\ -4 \\ 260 \\ -10 \end{pmatrix} \text{ [m] .} \quad (2)$$

Roughly, the chaser is located on a similar orbit to the target, 10 km behind in the flight direction. The complete rendezvous trajectory, including the far range approach and the inspection phase, is presented on Fig. 2. The left plot shows a 3D view of the trajectory of the chaser with respect to the target in the RTN frame, while the right plot is a 2D projection of this trajectory in the cross-track plane. The approach is performed autonomously by the GNC system, making use of the simulated line-of-sight measurements and performing impulsive maneuvers as described in Section II-C.

Once in proximity to the target, the main goal of the inspection phase is to maximize the target observability from different viewing angles and meanwhile ensuring a minimum safety distance in cross-track. In Tab. III the sequence of the different safety ellipses (SE) and walking safety ellipses (WSE) commanded in the inspection phase of this scenario are presented. They ensure a step-by-step approach and inspection of target spacecraft.

TABLE II
COMMANDED PARAMETERS FOR THE DIFFERENT STAGES OF THE INSPECTION PHASE

	$a\delta\lambda$ [m]	$a\delta e_x$ [m]	$a\delta i_x$ [m]
SE1	0	150	150
SE2	0	75	75
WSE1	-100	75	75
SE3	-100	25	25
WSE2	100	25	25
SE4 (inverse)	100	-25	-25
WSE3	-100	-25	-25

At the end of this rendezvous phase the chaser reaches the SE1 ("wide ellipse"). The dimension of SE1 (and also for the next two safety ellipses) is defined by the relative eccentricity vector norm in the RT plane, and by the relative inclination vector norm in cross-track (RN) direction. At this stage an initial fly-around maneuver is important to get an assessment of the target object and to ensure that the close-up inspection excludes a risk of collision. Thereafter, the SE1 narrows down to SE2 ("mid ellipse"), aiming to reduce the distance between the chaser and target. With WSE 1, the chaser drifts along-track in front of the target and starts to observe it from different distances. At the end of WSE 1, the distance to the target is reduced in RN plane and the chaser moves on SE3 ("close ellipse"). At this stage, the close-up examination of the target's features and detection of possible anomalies could be performed, while drifting within WSE2 as presented in the left image in Fig. 3.

Because daytime and the absence of blinding always happens at the same time on the relative orbit, the target satellite can always only be observed from the same side. This is illustrated on the left trajectory of Fig. 3, where the observation of the target is only possible on the purple parts of the inspection ellipse. Therefore, to gather observations of the target from the other side, it is suggested to perform an "ellipse inversion" by inverting the relative eccentricity and inclination vectors $a\delta e$ and $a\delta i$. By doing that, the blind zones will be located on the other part of the relative orbit, ensuring at the end a full observability of the target. Starting from SE4, the chaser is able to scan the target from the other side as seen in Fig. 3 (right), moving along WSE3.

The ΔV budget spent during each phase is presented in Tab. III. The highest budget of 0.4194 m/s was needed for autonomously bringing the chaser from far-range to the first safety ellipse. The ΔV needed to move along walking safety ellipses is 0.0165 m/s for WSE2 and 0.0514 m/s for WSE3.

TABLE III
ΔV COSTS DURING EACH PHASE

Maneuver	ΔV, m/s
far-range to SE1	0.4194
SE1 to SE2	0.1256
SE2 to WSE1	0.0107
WSE1 to SE3	0.0829
SE3 to WSE2	0.0165
WSE to SE4 (inversion)	0.0847
SE4 to WSE3	0.0514

IV. CONCLUSION

This paper presents the design of possible safe inspection trajectories around a target object in LEO orbit. The strategy enables to fly around the target and observe it from as many viewpoints as possible, taking into account the varying illumination and visibility conditions. The SiL far-range simulator serves here as an invaluable tool to test and to validate the whole rendezvous and fly-around stages. Our group is currently working on the improvement of the simulator, aiming to get a more precise on-ground simulation. Particularly, we are creating an image simulator to produce images for the far-range navigation. This image simulator will create an image of the stars and the target satellite, and come along with an image processing technique that enables to retrieve line-of-sight measurements from the images. Moreover, different error models will be added to the dynamics simulator to increase the realism of the whole testing environment.

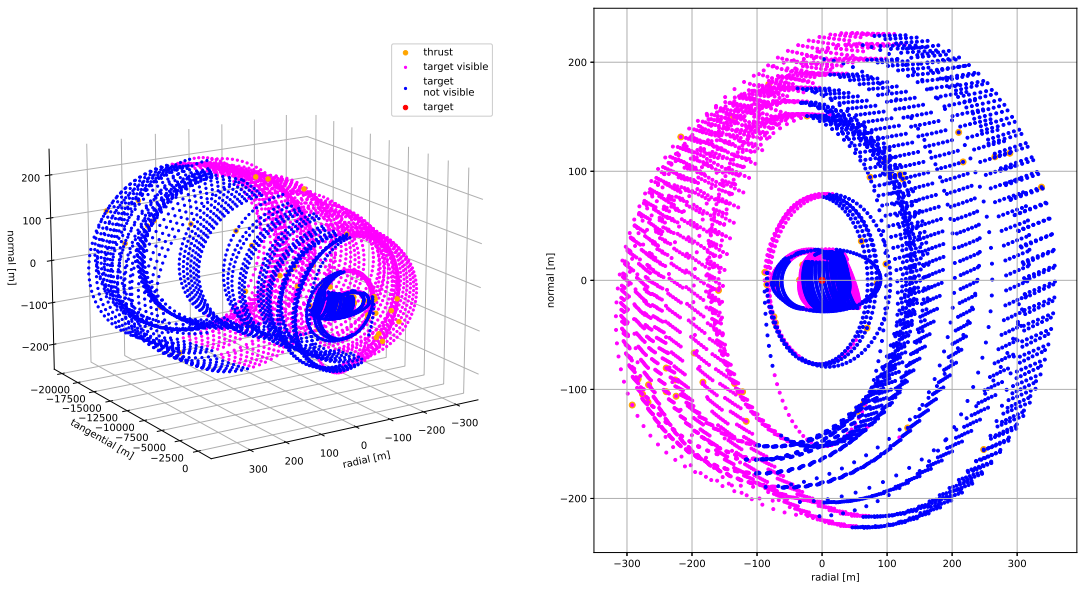

Fig. 2. Far-range rendezvous and inspection trajectories

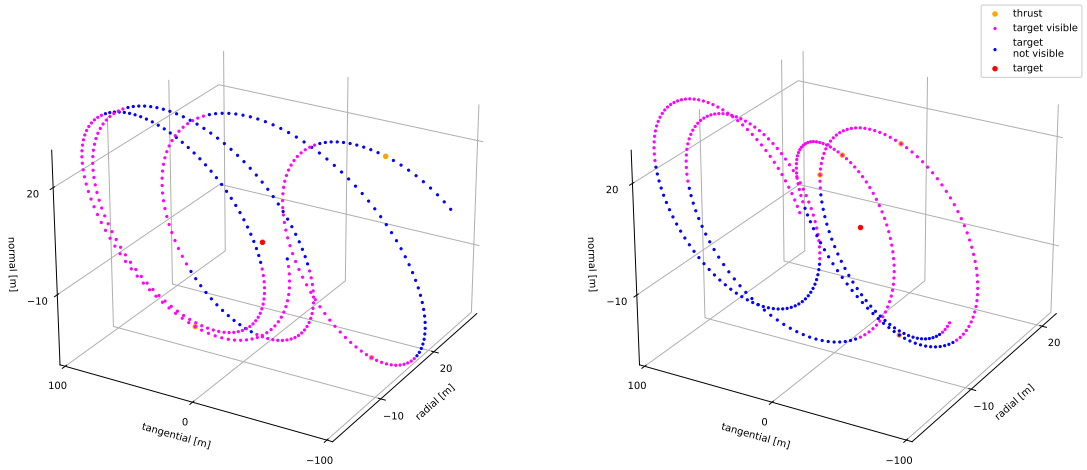

Fig. 3. Inspection trajectories, possible target view from all sides

REFERENCES

[1] J.-S. Ardaens, G. Gaias. Flight demonstration of spaceborne real-time angles-only navigation to a noncooperative target in low earth orbit. *Acta Astronautica*, vol. 153, pp. 367-382, 2018.

[2] W. Fehse. Rendezvous with and Capture / Removal of Non-Cooperative Bodies in Orbit: The Technical Challenges. *Journal of Space Safety Engineering*, vol. 1, pp. 17-27, 2014.

[3] Astroscale. https://astroscale.com/missions/adras-j/. Last accessed on 01.03.2024

[4] RocketLab. On Closer Inspection. https://www.rocketlabusa.com/missions/missions-launched/on-closer-inspection/. Last accessed on 01.03.2024.

[5] True Anomaly. https://www.trueanomaly.space/. Last accessed on 01.03.2024.

[6] Program Solicitation DARPA-PS-16-01 for Robotic Servicing of Geosynchronous Satellites (RSGS).

[7] Mission Extension Vehicle (MEV). https://cdn.prd.ngc.agencyq.site/-/media/wp-content/uploads/Mission-Extension-Vehicle-MEV-fact-sheet.pdf. Last accessed on 01.03.2024.

[8] F. Rems, H. Frei, E.-A. Risse, M. Burri. 10-Year Anniversary of the European Proximity Operations Simulator 2.0 - Looking Back at Test Campaigns, Rendezvous Research and Facility Improvements. *Aerospace*, 2021.

[9] NASA's Johnson Space Center high-fidelity Rendezvous, Proximity Operations and Docking. https://www.nasa.gov/reference/jsc-rendezvous-prox-ops-docking-subsystems/

[10] G. Borelli, G. Gaias, C. Colombo. Rendezvous and proximity operations design of an active debris removal service to a large constellation fleet. *Acta Astronautica*, vol.5, pp. 33-46, 2023.

[11] S. Silvestrini, J. Prinetto, G. Zanotti, M. Lavagna. Design of Robust Passively Safe Relative Trajectories for Uncooperative Debris Imaging in Preparation to Removal. *AAS/AIAA Astrodynamics Specialist Conference*, 2020.

[12] H. Zhuojun, J. Bohan, D. Zhaohui. Relative orbit design of CubeSats for on-orbit visual inspection of China space station. *Advances in Space Research*, vol. 73, 2024.

[13] G. Gaias, J.-S. Ardaens. Flight Demonstration of Autonomous Noncooperative Rendezvous in Low Earth Orbit. *Journal of Guidance, Control, and Dynamics*, vol. 41, no. 6, pp. 1137–1354, 2018.

[14] E. Gill, S. D'Amico, O. Montenbruck. Autonomous Formation Flying for the PRISMA Mission. *AIAA Journal of Spacecraft and Rockets*, 44/3, p.p. 671-681, 2007.

[15] P. Bodin, R. Noteborn, R. L. Nordström, T. Karlsson, S. D'Amico, J.-S. Ardaens, M. Delpech, J.C. Berges. Prisma Formation Flying Demonstrator: Overview and Conclusions from the Nominal Mission. *Advances in the Astronautical Sciences*, 2012.

[16] O. Montenbruck, E. K. A. Gill. Satellite Orbits: Models, Methods and Applications. Springer Science and Business Media, ISBN 354067280X, 9783540672807 2000.

[17] G. Gaias, S. D'Amico, J.-S. Ardaens. Angles-only navigation to a noncooperative satellite using relative orbital elements. *J. Guid. Control Dyn.*, 2014.

[18] G. Gaias, S. D'Amico, J.-S. Ardaens. Generalized Multi-Impulsive Maneuvers for Optimum Spacecraft Rendezvous in Near-Circular Orbit. *International Journal of Space Science and Engineering*, Vol. 3, No. 1, pp. 68–88, 2015.

[19] S. D'Amico, Autonomous formation flying in low earth orbit. *Technical University of Delft*, 2010.

[20] S. D'Amico, O. Montenbruck. Proximity operations of formation-flying spacecraft using an eccentricity/inclination vector separation. *J. Guid. Control Dyn.*, 29, 3, pp. 554–563, 2006.

[21] L. Renaut, H. Frei, A. Nüchter. Lidar pose tracking of a tumbling spacecraft using the smoothed normal distribution transform. *Remote Sensing*, vol. 15, no 9, p. 2286, 2023.